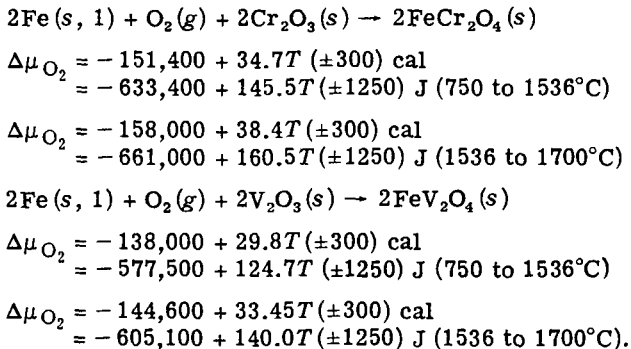


The Oxygen Potential of the Systems Fe + FeCr₂O₄ + Cr₂O₃ and Fe + FeV₂O₄ + V₂O₃ in the Temperature Range 750-1600°C

K. T. JACOB AND C. B. ALCOCK

From electromotive force (emf) measurements using solid oxide galvanic cells incorporating ZrO₂-CaO and ThO₂-YO_{1.5} electrolytes, the chemical potentials of oxygen over the systems Fe + FeCr₂O₄ + Cr₂O₃ and Fe + FeV₂O₄ + V₂O₃ were calculated. The values may be represented by the equations:



At the oxygen potentials corresponding to Fe + FeCr₂O₄ + Cr₂O₃ equilibria, the electronic contribution to the conductivity of ZrO₂-CaO electrolyte was found to affect the measured emf. Application of a small 60 cycle A.C. voltage with an amplitude of 50 mv across the cell terminals reduced the time required to attain equilibrium at temperatures between 750 to 950°C by approximately a factor of two. The second law entropy of iron chromite obtained in this study is in good agreement with that calculated from thermal data. The entropies of formation of these spinel phases from the component oxides can be correlated to cation distribution and crystal field theory.

THE spinel phases play an important role in the oxidation of alloys, formation of inclusions in cast metals and in refining operations in pyrometallurgy. Accurate information on the thermodynamic properties of the spinel phases would permit a more precise description of these metallurgical phenomena. A normal spinel structure (MX₂O₄) can be described as a close-packed cubic arrangement of anions with one-eighth of the tetrahedral holes filled with M²⁺ cations and one-half of the octahedral holes filled with X³⁺ cations. At high temperatures, cations can exchange positions, the magnitude of cation mixing being determined by the difference in "site preference energies". Relationships between thermodynamic parameters and structural information would be useful both for the estimation of values where measurements are lacking, and for the evaluation of thermochemical data when a large body of experimental information is available.

The standard free energy of formation of iron chromite has been measured by Boericke and Bangert,¹ Kunnmann *et al.*,² Katsura and Muan,³ Novokhatski and Lenev,⁴ and Chen and Chipman,⁵ using gas-equilibrium methods, while solid oxide galvanic cells were em-

ployed by Tretjakow and Schmalzried,⁶ Rezukhina *et al.*,⁷ and Fruehan.⁸ The results show a spread of 8.6 kcal gr mole⁻¹ (36 kJ gr mole⁻¹) of chromite at 1000°C. Furthermore, the second law entropies obtained from the free energy measurements^{1-4,6,7} cannot be reconciled with the value obtained from thermal data.^{9,10}

The standard free energy of formation of iron vanadite has been measured by Kunnmann *et al.*,² below the melting point of iron, and by Chipman and Dastur,¹¹ Karasev *et al.*,¹² Narita,¹³ and Kay and Kontopoulos¹⁴ above the melting point. The values obtained by Chipman and Dastur¹¹ and Narita¹³ agree at 1600°C, while that of Karasev *et al.*,¹² is 3.7 kcal gr mole⁻¹ (15.5 kJ gr mole⁻¹) more positive and that of Kay and Kontopoulos¹⁴ is 1 kcal gr mole⁻¹ (4.18 kJ gr mole⁻¹) more negative. Extrapolation of these data to temperatures below the melting point of iron does not match the measurements of Kunnmann *et al.*,² It will be shown later that the temperature coefficients of the free energy of formation obtained from the data of Karasev *et al.*,¹² and Kay and Kontopoulos¹⁴ are not consistent with the current knowledge on the statistical thermodynamics of gases and condensed phases.

In an attempt to resolve the above discrepancies, the chemical potentials of oxygen over the mixtures Fe + FeCr₂O₄ + Cr₂O₃ and Fe + FeV₂O₄ + V₂O₃ were measured with solid oxide galvanic cells incorporating ZrO₂-CaO and ZrO₂-CaO in combination with ThO₂-

K. T. JACOB is Senior Research Associate, and C. B. ALCOCK is Chairman, Dept. Metallurgy and Materials Science, University of Toronto, Toronto, Canada, M5S 1A4.

Manuscript submitted July 19, 1974.

$\text{YO}_{1.5}$ as electrolyte, using $\text{Fe} + \text{FeO}$ and $\text{Mo} + \text{MoO}_2$ mixtures as reference electrodes, in the temperature range 750 to 1600°C.

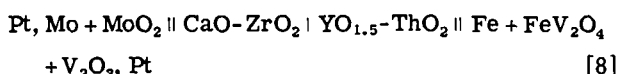
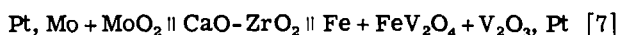
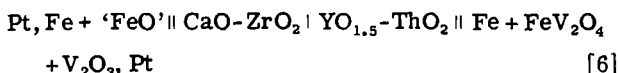
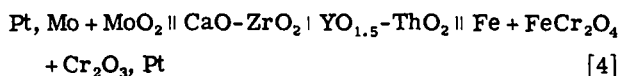
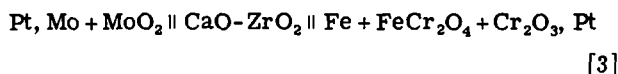
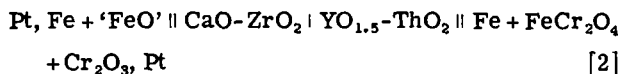
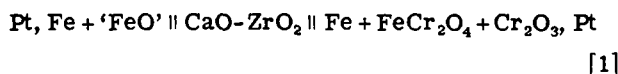
EXPERIMENTAL

Materials

The fine powders of metallic iron and ferric oxide used in this study were of spectrographic standard and were supplied by Johnson Matthey Chemicals. Chromium and vanadium oxides (Cr_2O_3 and V_2O_3) were obtained from Alfa Inorganics and were 99.9 pct pure. Iron chromite (FeCr_2O_4) and vanadite (FeV_2O_4) were prepared by prolonged heating at 1100°C for 3 to 4 days of pressed pellets containing Fe , Fe_2O_3 and Cr_2O_3 (or V_2O_3) in the molar ratio (1:1:3). The pellets were contained in alumina crucibles placed inside evacuated silica capsules. Formation of the ternary compounds was confirmed by X-ray diffraction analysis. Impervious calcia-stabilized zirconia tubes supplied by Zirconia Corporation of America contained 7.5 mole pct CaO . Thoria pellets doped with 15 mole pct yttria were prepared from mixed nitrate solutions by evaporation and subsequent decomposition. The resulting powder was pressed into pellets at a pressure of 30 tons sq in.^{-1} and sintered under an atmosphere of 90 pct N_2 + 10 pct H_2 at 1800°C. The argon gas used as the atmosphere for the emf runs was 99.98 pct pure and was dried and then deoxidized by passing through a column of titanium granules maintained at 900°C.

Apparatus and Procedure

The method of preparation of the electrodes was similar to that described earlier.¹⁵ Fine powders of component metals and oxides were mixed in equimolar proportions, compacted into pellets and sintered in evacuated quartz capsules at 1100°C. The apparatus and cell arrangements were identical to that used in an earlier study on iron aluminate.¹⁵ The voltages of the following cells were measured as a function of temperature:



Cells 1, 2, 5 and 6 were employed in the temperature

range 750 to 1200°C, and cells 3, 4, 7 and 8 from 950 to 1400°C. In bielectrolyte cells, the $\text{ThO}_2-\text{YO}_{1.5}$ electrolyte was placed in contact with the electrode having the lower oxygen partial pressure. The cell temperature was measured with a Pt/Pt-13 pct Rh thermocouple. The oxygen chemical potential over $\text{Fe} + \text{FeV}_2\text{O}_4 + \text{V}_2\text{O}_3$ at 1600°C was measured by dipping a closed end ZrO_2-CaO tube containing a $\text{Mo} + \text{MoO}_2$ reference electrode into 10 g of liquid iron equilibrated with 6 g of FeV_2O_4 and 4 g of V_2O_3 for 3 to 5 h. The liquid iron was contained in an alumina crucible, which was lined inside with V_2O_3 . Molybdenum wires were used to make electrical contact with liquid iron and the $\text{Mo} + \text{MoO}_2$ reference electrode. Similar experiments were not carried out with the $\text{Fe} + \text{FeCr}_2\text{O}_4 + \text{Cr}_2\text{O}_3$ system, since earlier studies^{11,18} have shown that the phases do not coexist under equilibrium conditions at 1600°C.

The emf was measured with either 'Solartron' or 'Keithley' digital voltmeters. The reversibility of the cells was checked by passing small external currents in either direction. In each case the emf was found to return to the original value. The time required to reach equilibrium (steady emf) varied from 16 h at 750°C to 2 h at 1400°C. The emf was also found to be independent of the flow rate of the inert gas. Application of an A.C. ripple with an amplitude of 50 mv was found to shorten the time required for equilibration in the temperature range 750 to 950°C by approximately a factor of two. In each case, the cell emfs were monitored for 2 to 6 h after the removal of the A.C. potential. Application of the A.C. potential at higher temperatures was found to accelerate the corrosion of the electrolyte by the $\text{Fe} + \text{FeO}$ electrode. The phases present in the electrode pellets were established before and after experiments by X-ray diffraction. These studies showed that no changes occurred in the electrodes during the experiments.

Results

The variation of the emf of cells 1 and 2 with temperature is shown in Fig. 1. The emf of cell 1 using the ZrO_2-CaO electrolyte was found to be 3 to 5 mv lower than that of cell 2, in which the $\text{ThO}_2-\text{YO}_{1.5}$ pellet was used adjacent to the $\text{Fe} + \text{FeCr}_2\text{O}_4 + \text{Cr}_2\text{O}_3$ electrode. The emf of cell 1 was found to decrease gradually with time. A trace of the time dependence of the emf at 1200°C, after passing an external current to remove oxygen from the $\text{Fe} + \text{FeCr}_2\text{O}_4 + \text{Cr}_2\text{O}_3$ electrode is shown in Fig. 2. The value of the 'plateau' emf was independent (± 3 mv) of the amount of current passed (5 to 100 μA for 15 min to 60 min). Following the method of Diaz and Richardson¹⁷ the emfs corresponding to the plateau may be taken to represent the equilibrium values, and are plotted in Fig. 1.

The temperature dependences of the emf of cells 3, 4, 7 and 8 are shown in Fig. 3. Again the emf of cell 3 is 2 to 6 mv below that of cell 4. The emf of cells 2, 4, 5, 6, 7 and 8 were reproducible on repeated temperature cycling. The difference in the emf of cells 1 and 2, 3 and 4, may be attributable to the onset of electronic conductivity in the ZrO_2-CaO electrolyte at the oxygen partial pressures corresponding to the three phase equilibrium $\text{Fe} + \text{FeCr}_2\text{O}_4 + \text{Cr}_2\text{O}_3$. The values of the emf of cells 5 and 6 shown in Fig. 4 are the

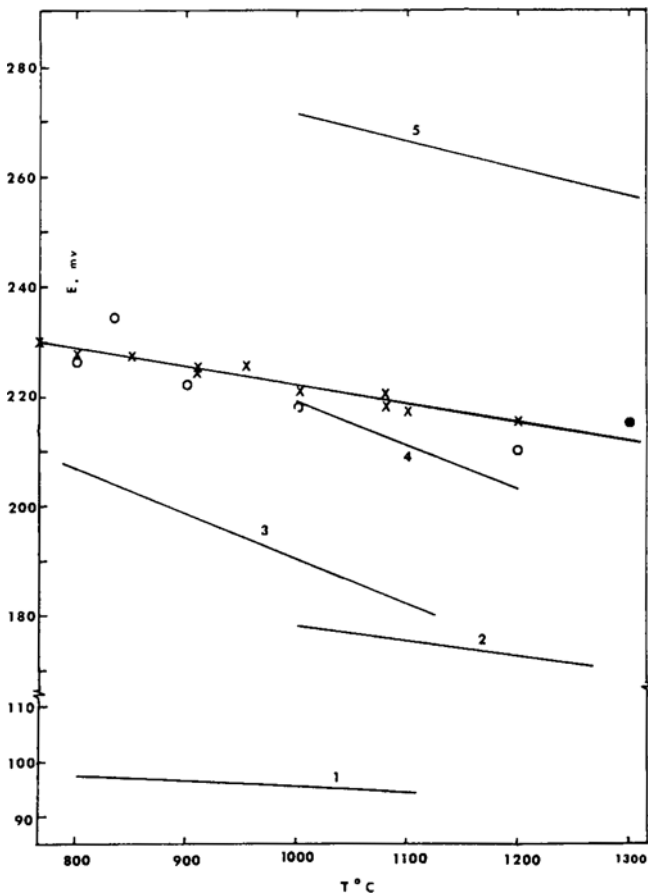


Fig. 1—The temperature dependence of the emf of cell 1 (○) and cell 2 (×) obtained in this study. 1 Kunmann *et al.*,² 2 Boericke and Bangert,¹ 3 Tretjakow and Schmalzried,⁶ 4 Rezukhina *et al.*,⁷ 5 Novokhatski and Lenev,⁴ ● Katsura and Muan.³

same within experimental error (± 3 mv). These results indicate that at the oxygen potential corresponding to the $\text{Fe} + \text{FeV}_2\text{O}_4 + \text{V}_2\text{O}_3$ equilibrium, there is no significant electronic contribution ($t_e < 0.01$) to the conductivity of $\text{ZrO}_2\text{-CaO}$. The temperature dependence of the emf for the various cells can be represented by the equations,

$$E_2 = 270 - 3.75 \times 10^{-2}T \text{ mv}$$

$$E_4 = 138 + 5.72 \times 10^{-2}T \text{ mv}$$

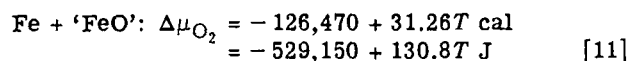
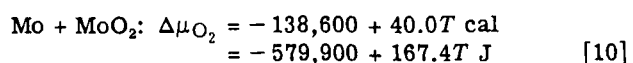
$$E_5 = E_6 = 125.2 + 1.583 \times 10^{-2}T \text{ mv}$$

$$E_7 = E_8 = -6.3 + 11.06 \times 10^{-2}T \text{ mv.}$$

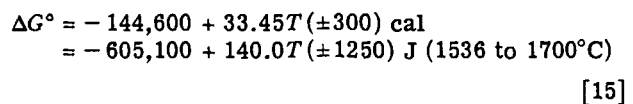
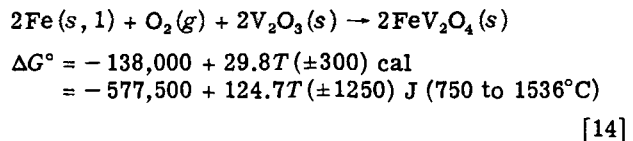
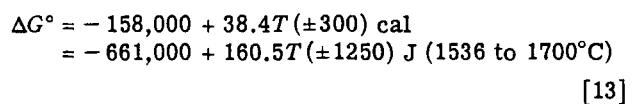
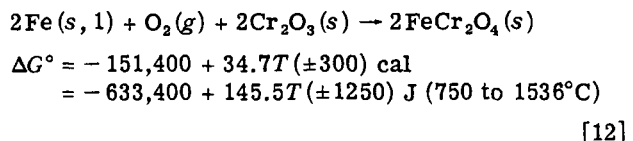
The emf of cell 7 was $200 (\pm 4)$ mv at 1600°C and $194 (\pm 4)$ mv at 1589°C . The emfs above the melting point of iron were constant for 5 to 10 min after immersion of the electrolyte tube. The difference in oxygen potential between the two electrodes is related to the emf by the relation

$$\Delta\mu_{\text{O}_2} = RT \ln \frac{p'_{\text{O}_2}}{p''_{\text{O}_2}} = -4FE \quad [9]$$

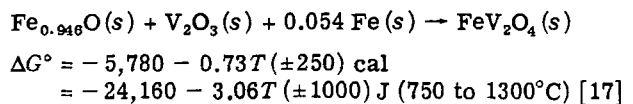
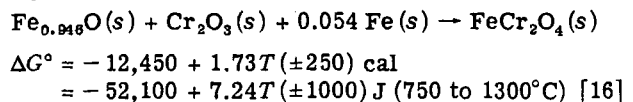
where $F = 23,063 \text{ cal V}^{-1} \text{ mole}^{-1}$, E is the emf in volts and the chemical potential is expressed in cal. The oxygen potential corresponding to the reference electrodes are given by the equations,^{15,18}



When Eqs. [9], [10] and [11] are combined with the measured emf, the following equations are obtained for the oxygen potential of the three phase mixtures:



Throughout this paper $\text{cal} = 4.184 \text{ J}$. For the purpose of internal consistency and in view of the uncertainty limits, four significant figures are used for representing the numerical terms in the above equations. The quoted uncertainty limits on the standard free energy changes were obtained by combining the uncertainties in measured emf and the oxygen potential of the reference electrodes. The equations for the temperature range 1536 to 1700°C are derived by using the heat of fusion of iron¹⁹ (3.3 kcal or 13.8 kJ). The values obtained in this manner for $\text{Fe} + \text{FeV}_2\text{O}_4 + \text{V}_2\text{O}_3$ are in good agreement with the direct measurements at 1600°C . Strictly, the variation of the free energy with temperature in the range 750 to 1536°C should exhibit small changes in slope at points corresponding to the solid-state phase transitions in iron. However, the results using $\text{Fe} + \text{'FeO}'$ and $\text{Mo} + \text{MoO}_2$ reference electrodes agree within the experimental error (± 3 mv) and indicate that a linear equation may be used for this temperature range. The iron chromite and vanadate phases might exhibit nonstoichiometry; the values quoted in this study correspond to the Cr_2O_3 or V_2O_3 saturated compositions. The following equations characterize the formation of the spinel phases from the component oxides:



DISCUSSION

The results obtained in this study for iron chromite are compared with those reported in the literature in

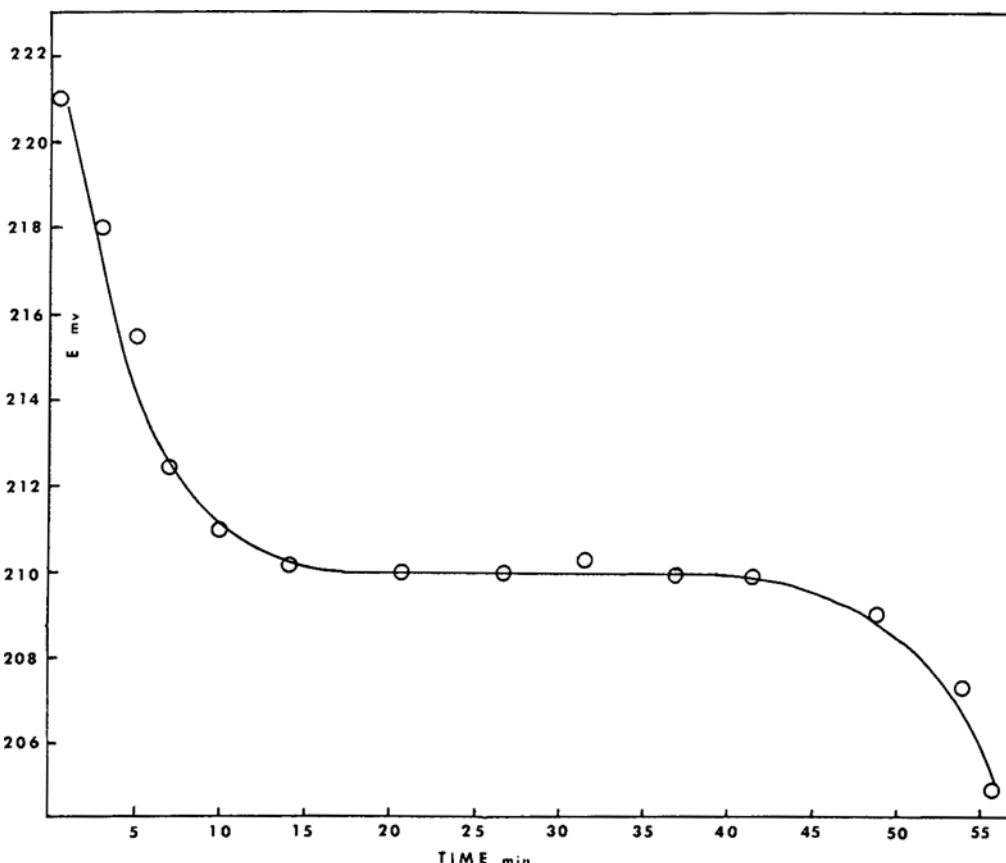


Fig. 2—The time dependence of the emf of cell 1 at 1200°C.

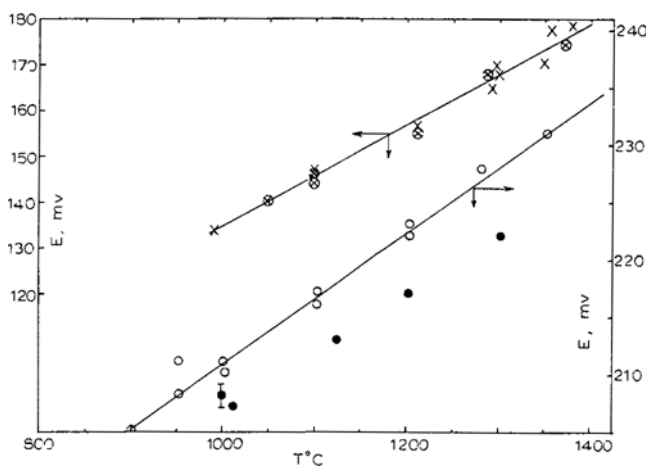


Fig. 3—The variation of emf with temperature: ● cell 3; ○ cell 4; □ cell 7; × cell 8.

Fig. 1. Values reported by Katsura and Muan,³ and Rezukhina *et al.*⁷ are in fair agreement with the results of this study. Tretjakow and Schmalzried⁶ used a calcia stabilized zirconia electrolyte and air as the reference electrode. The presence of electronic conduction in the electrolyte would explain the lower emfs obtained in their study. Kunmann *et al.*² measured the CO/CO₂ ratio required for the synthesis of the chromite from iron and chromium sesquioxide. The presence of kinetic restrictions on the formation reaction would require the presence of a more oxidizing gas mixture for the synthesis than that observed under equilibrium conditions. The oxygen potential obtained from Kun-

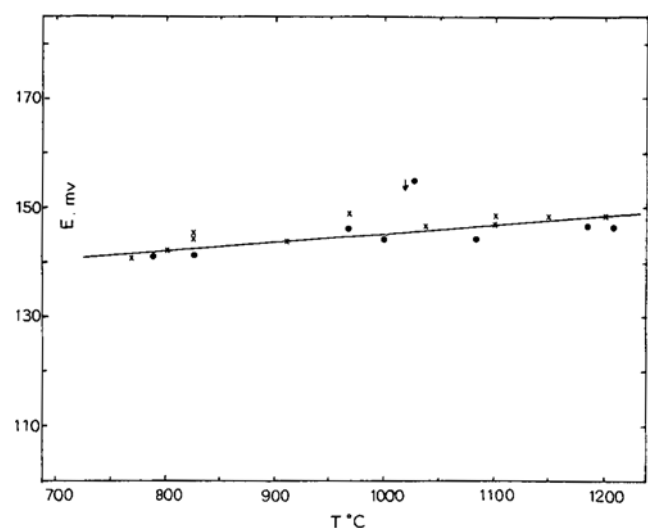
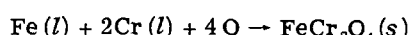


Fig. 4—The temperature dependence of emf of cells 5 (●) and 6 (×).

mann *et al.* is considerably more positive and suggests that these measurements may not reflect equilibrium conditions. No obvious reasons can be found for the discrepancy between the present results and those of Boericke and Bangert,¹ and Novokhatski and Lenev.⁴

Chen and Chipman⁵ and Fruehan⁸ have measured the free energy change at 1600°C for the reaction



where O denotes oxygen dissolved in liquid iron. Their

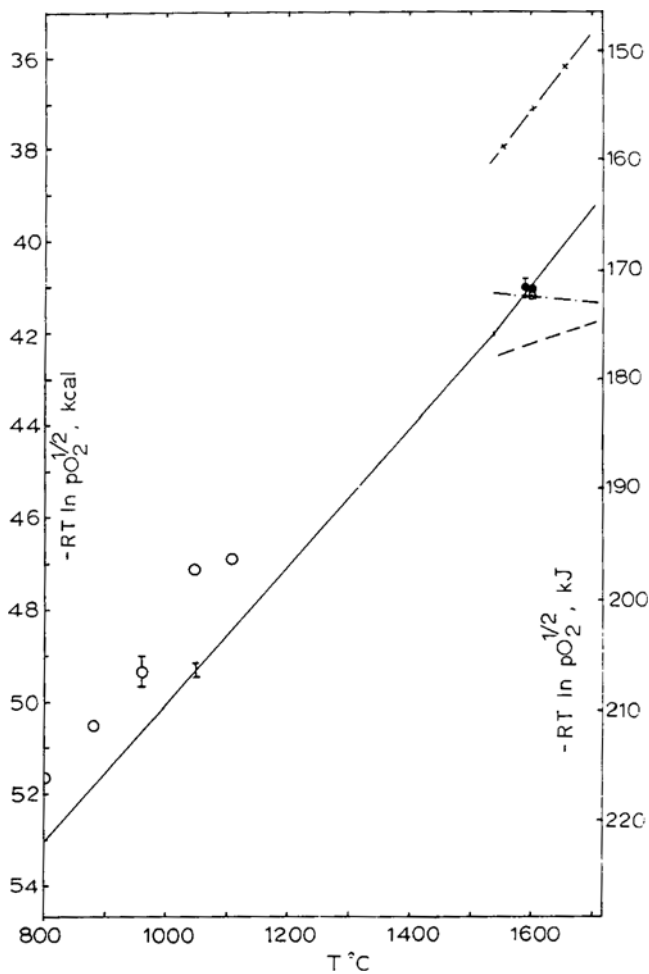
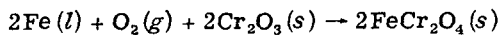


Fig. 5—The variation of $RT \ln pO_2^{1/2}$ with temperature for the system $Fe + FeV_2O_4 + V_2O_3$:

—●— this study; - - - Narita;¹³
 - - - - Kay and Kontopoulos;¹⁴
 - - × - Karasev *et al.*,¹² ○ Kunmann *et al.*,²
 □ Chipman and Dastur.¹¹

values are combined with the free energy of solution of oxygen in iron,²⁰ the free energy of formation of Cr_2O_3 ,²¹ and the free energy of fusion of Cr¹⁹ to obtain the free energy change for the reaction,



$$\Delta G_{1873}^{\circ} = -85,430 \text{ cal} \quad \left. \begin{array}{l} \\ = -357,450 \text{ J} \end{array} \right\} \text{Chen and Chipman}$$

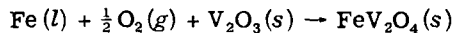
$$\Delta G_{1873}^{\circ} = -82,370 \text{ cal} \quad \left. \begin{array}{l} \\ = -344,626 \text{ J} \end{array} \right\} \text{Fruehan.}$$

These values compare with a value of $-86,100 (\pm 300)$ cal ($-360,400 \text{ J}$) obtained from the results of this study (Eq. [13]).

The heat capacity measurements of Shomate⁹ (53 to 298 K) and Naylor¹⁰ (298 to 1780 K) can be used to calculate a value of $93.56 (\pm 0.6) \text{ cal deg}^{-1} \text{ mole}^{-1}$ for the entropy of $FeCr_2O_4$ at 1300 K. The second law entropy of formation of $FeCr_2O_4$ (Eq. [12] or [16]) obtained in this study can be combined with the entropy of $Cr_2O_3(s)$, $Fe(s)$ and $O_2(g)$ or ' $FeO(s)$ '¹⁹ to give a value of $94.17 (\pm 1.0) \text{ cal deg}^{-1} \text{ mole}^{-1}$ or $394 \text{ J deg}^{-1} \text{ mole}^{-1}$ at 1300 K. The second law entropy of $FeCr_2O_4$ is in good agreement with that calculated from thermal data. The third

law heat of formation of $FeCr_2O_4$ at 298 K is $-11,800 (\pm 350) \text{ cal mole}^{-1}$ or $-49,370 (\pm 1,460) \text{ J mole}^{-1}$.

The oxygen potential over the $Fe + FeV_2O_4 + V_2O_3$ system is plotted in Fig. 5. The values reported by other investigators are also shown for comparison. The results of this study are in good agreement with the measurements of Chipman and Dastur¹¹ and Narita¹³ at 1600°C. The temperature dependence of the oxygen potential is negative according to Narita.¹³ This is not in accord with the statistical thermodynamics of gases and condensed phases. For the reaction,



the main contribution to the entropy change arises from the entropy of the gaseous reactant, which combines with the solid phases to form a solid product. The entropy change would therefore be negative and greater than $10 \text{ cal deg}^{-1} \text{ mole}^{-1}$ ($42 \text{ J deg}^{-1} \text{ mole}^{-1}$). The free energy of formation of FeV_2O_4 obtained by Karasev *et al.*¹² is 3.7 kcal (15.5 kJ) more positive than that obtained in this study. The results of Kay and Kontopoulos¹⁴ are 1.3 to 2.7 kcal (5.4 to 11.3 kJ) more negative and the temperature coefficient of their free energy indicates an entropy change of $-4.4 \text{ cal deg}^{-1} \text{ mole}^{-1}$ ($18.4 \text{ J deg}^{-1} \text{ mole}^{-1}$). The free energy of formation of FeV_2O_4 obtained by Kunmann *et al.*² at lower temperatures is 1.3 kcal (5.4 kJ) more positive than that obtained in this study. As discussed earlier, this discrepancy probably arises from kinetic restrictions in the synthesis of FeV_2O_4 from Fe , V_2O_3 and $CO + CO_2$ mixtures.

ENTROPY OF FORMATION OF SPINELS

Since the entropy arising from the mixing of cations in the tetrahedral and octahedral sites of the spinel structure would make a significant contribution to the total entropy of a spinel at high temperatures, information on the cation distribution is required to account for the entropies of formation of spinels from component oxides which were obtained in this study. Dunitz and Orgel²² have discussed the distribution of transition-metal ions among tetrahedral and octahedral sites in oxides from the viewpoint of crystal field theory. When a transition-metal ion is surrounded by an octahedron of negative ions, the d orbitals are split by the electrostatic field into a triply degenerate t_{2g} orbital which is stabilized and a doubly degenerate e_g orbital which is destabilized relative to the mean d orbital. In the tetrahedral field, the situation is similar but the e_g orbitals are more stable than the t_{2g} orbitals. Dunitz and Orgel²² have calculated the magnitude of the stabilization energies for the transition-metal ions in tetrahedral and octahedral sites from optical and magnetic measurements. The difference between the stabilization energies in the two competing sites gives the 'site preference energy', which is shown in Table I. If the mixing of cations on each type of site is ideal, the cation distribution can be obtained by equating the difference in octahedral site preference energy for the two cations to the product of absolute temperature and the ideal entropy of mixing.

Navrotsky and Kleppa²³ have used the mass-action law treatment to derive an empirical scale of octahedral site preference energies from available high

Table I. Octahedral Site Preference Energies for Various Ions from Crystal Field Theory²²

Ion	Octahedral Site Preference Energy	
	kcal	kJ
Fe ²⁺	-4.0	-16.7
Ni ²⁺	-20.6	-86.2
Co ²⁺	-7.4	-31.0
Cu ²⁺	-15.2	-63.6
Mn ²⁺	0	0
V ³⁺	-12.8	-53.6
Cr ³⁺	-37.7	-157.7
Fe ³⁺	0	0
Al ³⁺	(-18.6)*	(-77.8)*

*Based on the value for Ni²⁺ and measured cation distribution in NiAl₂O₄.

Table II. Cation Distribution in Spinels

Spinel (MX ₂ O ₄)	ΔH _{ex}		Cation Distribution: Fraction of M on Tetrahedral Site (x)	
	kcal	kJ	Calculated 1200 K	Measured
FeAl ₂ O ₄	14.6	61.1	0.936	0.923 (1473 K) ²⁴
NiAl ₂ O ₄	-2.0	-8.4	0.21	0.20 (1300 K) ²⁵
CoAl ₂ O ₄	11.2	46.9	0.89	0.95 (1123 K) ^{24,25}
CuAl ₂ O ₄	3.4	14.2	0.54	0.4 (1100 K) ²⁶
MnAl ₂ O ₄	18.6	77.8	0.972	0.958 (1272 K) ²⁴
FeV ₂ O ₄	8.8	36.8	0.81	—
FeCr ₂ O ₄	33.7	141	0.999	—
FeFe ₂ O ₄	-4.0	-16.7	0.11	—

temperature crystallographic information on cation distribution in spinels and a value for Al³⁺ obtained from calorimetric data on the transformation of α -alumina to γ -alumina. However, lack of accurate cation distribution data on vanadites, prevents the estimation of an octahedral site preference energy of V³⁺ using this procedure. Although the values on Navrotsky and Kleppa's empirical scales are generally about 8 to 10 kcal (33.5 to 42 kJ) more negative for a given cation than those obtained from crystal field theory, the difference in the energy values for two cations (which determines the distribution) is approximately the same on both scales.

The values for octahedral site preference energy from crystal field theory were used to compute the cation distribution in FeV₂O₄ and FeCr₂O₄. The value for Al³⁺ in Table I is obtained relative to that for Ni²⁺ using the measured equilibrium distribution of Ni²⁺ and Al³⁺ in NiAl₂O₄ at 1300 K.²⁵ In a spinel crystal of the composition $M_x X_{1-x} [M_{(1-x)} X_{(1+x)}] O_4$ in thermal equilibrium, the free energy change for the exchange reaction, $M + [X] \rightarrow [M] + X$, is zero. The change in enthalpy for the exchange reaction can therefore be equated to the product of absolute temperature and change in configurational entropy. The partial molar entropy of a cation on any site is equal to $-R \ln N_i$, where N_i is the mole ionic fraction of the cation i on that site

$$\Delta H_{ex} = -RT \ln \frac{N_i [M] N_X}{N_i [X] N_M} = -RT \ln \frac{(1-x)^2}{x(1+x)} \quad [18]$$

where [] indicates atoms in octahedral position and

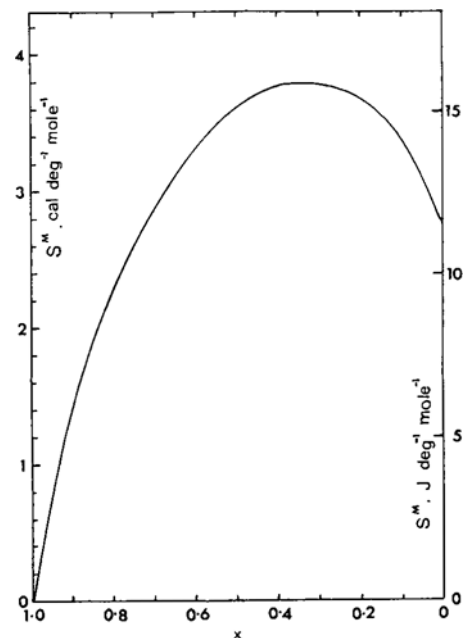


Fig. 6—The configurational entropy of mixing of cations in 2-3 spinels; x is the fraction of divalent cation in tetrahedral site.

Table III. Comparison of Entropies and Heats of Formation with Entropies of Mixing of Cations of Spinels Containing Fe²⁺

Spinel	ΔS*		ΔS ^M		ΔH*	
	cal deg ⁻¹ mole ⁻¹	J deg ⁻¹ mole ⁻¹	cal deg ⁻¹ mole ⁻¹	J deg ⁻¹ mole ⁻¹	kcal mole ⁻¹	kJ mole ⁻¹
FeFe ₂ O ₄ (Fe ₃ O ₄)	1.47 ²⁷	6.15 ²⁷	3.42	14.31	-5.1 ²⁷	-21.3 ²⁷
FeV ₂ O ₄	0.73	3.05	2.20	9.20	-5.78	-24.2
FeAl ₂ O ₄	-0.78 ¹⁵	-3.26 ¹⁵	1.04	4.35	-6.66 ¹⁵	-27.9 ¹⁵
FeCr ₂ O ₄	-1.73	-7.24	0.03	0.13	-12.45	-52.1

*For the reaction $Fe_{0.95}O(s) + 0.05 Fe(s) + X_2O_3(s) \rightarrow FeX_2O_4(s)$.

x is the fraction of divalent metal M in tetrahedral position. The exchange energies derived from the values in Table I for various spinels are shown in Table II, along with calculated cation distribution at 1200 K. Comparison of the calculated cation distribution with crystallographic information (Table II) illustrates the accuracy of the estimations. The extent of cation mixing increases from FeCr₂O₄ to FeAl₂O₄ and FeV₂O₄. The configurational entropy of mixing of cations may be calculated using Temkin's ionic fraction approach,²³

$$\Delta S^M = -R \left[x \ln x + (1-x) \ln (1-x) + (1-x) \ln \frac{(1-x)}{2} + (1+x) \ln \frac{(1+x)}{2} \right]. \quad [19]$$

The variation of ΔS^M with x is illustrated in Fig. 6. The mixing contribution to the entropy of the three spinel phases containing Fe²⁺ are shown in Table III, along with their entropies of formation from component oxides obtained in this study. It is apparent that the differences in the measured entropies of formation are mainly due to differences in cation distribution and the corresponding mixing entropies.

This close correspondence probably arises from the fact that the differences in lattice parameter and the degree of covalent bonding in the three Fe²⁺ spinels

are paralleled by corresponding differences in the properties of the trivalent oxides which have the corundum structure. It is also clear from Fig. 6 that drop calorimetric techniques for heat capacity measurements would not be suitable in computing entropies at high temperatures of spinels with significant cation mixing. The disorder on the cation sites increases with temperature, and the entropies obtained in this study are average values for the temperature range covered.

The heat of formation of the spinel phases from component oxides shown in Table III decreases with increasing cation mixing. This is in line with the calculations of Verwey *et al.*,²⁸ who have shown that Madelung constant and electrostatic stability decrease as the fraction of M^{2+} ions in octahedral position increases. The Madelung constant is also sensitive to the oxygen parameter,²⁹ u , which is a measure of the departure from the ideal spinel structure. Unfortunately, the values for this parameter are not known accurately for all the phases listed in Table III.

SUMMARY AND CONCLUSIONS

1) Solid oxide galvanic cells were used to measure the oxygen potential of the three phase mixtures $Fe + FeCr_2O_4 + Cr_2O_3$ and $Fe + FeV_2O_4 + V_2O_3$ in the temperature range 750 to 1600°C. The second law entropy of formation of $FeCr_2O_4$ obtained in this study is in good agreement with that calculated from thermal data.

2) Application of a small A.C. potential (50 mv) across the cell terminals was found to decrease the time required to attain equilibrium in the temperature range 750 to 950°C.

3) At the oxygen potentials corresponding to the $Fe + FeCr_2O_4 + Cr_2O_3$ equilibria, electronic contributions to the conductivity of $CaO-ZrO_2$ electrolyte were found to affect the measured emf.

4) The cation distribution in spinel phases at high temperatures can be evaluated from 'site preference energies' derived from crystal field theory. The entropy of formation of spinel phases from the component oxides with rock salt and corundum structures may be expressed as $-1.75 + \Delta S^M_{cal} \text{ deg}^{-1} \text{ mole}^{-1}$ or $-7.25 + \Delta S^M \text{ J deg}^{-1} \text{ mole}^{-1}$, where ΔS^M is the entropy of mixing of cations.

ACKNOWLEDGMENT

This work was carried out as part of the Electrochemical Sensors project which has been funded by the National Research Council of Canada.

REFERENCES

1. F. G. Boericke and W. M. Bangert: *Bur. Mines (U.S.) Rep. Invest.*, 1945, N. 3813.
2. W. Kunmann, D. B. Rogers, and A. Wold: *J. Phys. Chem. Solids*, 1963, vol. 24, p. 1535-38.
3. T. Katsura and A. Muan: *Trans. TMS-AIME*, 1964, vol. 230, p. 77.
4. I. A. Novokhatski and L. M. Lenev: *Zh. Neorg. Khim.*, 1966, vol. 11, p. 2014.
5. H. M. Chen and J. Chipman: *Trans. ASM*, 1947, vol. 38, p. 70-113.
6. J. D. Tretjakow and H. Schmalzried: *Ber. Bunsenges. Phys. Chem.*, 1965, vol. 69, p. 396.
7. T. N. Rezukhina, V. A. Levitski, and B. A. Istomin: *Electrochemistry* (Russian), 1965, vol. 1, p. 467-71.
8. R. J. Fruehan: *Trans. TMS-AIME*, 1969, vol. 245, p. 1215-18.
9. C. H. Shomate: *Ind. Eng. Chem.*, 1944, vol. 36, p. 910.
10. B. F. Naylor: *Ind. Eng. Chem.*, 1944, vol. 36, p. 933.
11. J. Chipman and M. Dastur: *Trans. AIME*, 1951, vol. 191, p. 111-15.
12. R. A. Karasev, A. Y. Polyakov, and A. M. Samarin: *Dokl. Akad. Nauk USSR*, 1952, vol. 85, pp. 1313-16.
13. K. Narita: *Nippon Kagaku Zasshi*, 1958, vol. 79, pp. 866-72.
14. D. A. R. Kay and A. Kontopoulos: *Proceedings of the International Symposium on Metallurgical Chemistry: Applications in Ferrous Metallurgy*, 'Sheffield, England, 1971.
15. J. C. Chan, C. B. Alcock, and K. T. Jacob: *Can. Met. Quart.*, 1973, vol. 12, pp. 439-43.
16. D. C. Hiltz, W. J. Forgeng, and R. L. Folkman: *J. Metals*, 1955, vol. 7, p. 253.
17. C. M. Diaz and F. D. Richardson: *Trans. Inst. Mining Met.*, (London), 1967, vol. 76, C196-203.
18. C. B. Alcock and J. C. Chan: *Can. Met. Quart.*, 1972, vol. 11, p. 559.
19. O. Kubaschewski, E. L. Evans, and C. B. Alcock: *Metallurgical Thermochemistry*, Pergamon Press, 1967.
20. J. F. Elliott, M. Gleiser, and V. Ramakrishna: *Thermochemistry for Steel-making*, vol. II, Addison-Wesley, 1964.
21. Y. Jeannin, C. Mannerskantz, and F. D. Richardson: *Trans. AIME*, 1963, vol. 227, p. 300.
22. J. D. Dunitz and L. E. Orgel: *J. Phys. Chem. Solids*, 1957, vol. 3, pp. 318-23.
23. A. Navrotsky and O. J. Kleppa: *J. Inorg. Nucl. Chem.*, 1967, vol. 29, p. 2701.
24. W. W. Roth: *J. Phys.*, 1964, vol. 25, p. 507.
25. H. Schmalzried: *Z. Phys. Chem. Frankf., Aust.*, 1961, vol. 28, p. 203.
26. F. Bertaut: *Compt. Rend.*, 1954, vol. 239, p. 504.
27. D. R. Stull *et al.*: JANAF Thermochemical Tables, NSRDS-NBS 37, 1971.
28. E. J. W. Verwey, F. DeBoer, and J. H. van Santen: *J. Chem. Phys.*, 1948, vol. 16, pp. 1091-92.
29. F. DeBoer, J. H. van Santen, and E. J. W. Verwey: *J. Chem. Phys.*, 1950, vol. 18, pp. 1032-34.